



Isospin asymmetric matter in uniform and nonuniform strong magnetic fieldsYuan Wang  and Xin-Jian Wen *Institute of Theoretical Physics, Shanxi University, Taiyuan, Shanxi 030006, China*

(Received 8 August 2023; accepted 18 December 2023; published 8 January 2024)

Isospin asymmetric quark matter is investigated with the Polyakov Nambu–Jona-Lasinio model at zero temperature in a strong magnetic field. The isospin symmetry/asymmetry can be controlled by altering the fraction parameter α of the two kinds of interactions, i.e., the scalar coupling and instanton-induced coupling. Specially, the flavor decoupled state with $\alpha = 0$ is strongly isospin asymmetric. It is accompanied by the discrepancy of the u and d quarks in the chiral phase transitions, which is eliminated up to $\alpha = 0.5$. It is found that there exists a critical value α_c , above which the simultaneous chiral restoration would happen for the flavor isodoublet, no matter whether their masses are equal or not. The α_c can be decreased by the increase of the magnetic field. Finally, it is suggested that the presence of the Polyakov potential increases the maximum central magnetic field of compact stars up to 3.5×10^{18} G.

DOI: [10.1103/PhysRevC.109.015201](https://doi.org/10.1103/PhysRevC.109.015201)**I. INTRODUCTION**

The study of the quantum chromodynamics (QCD) phase diagram attracts a lot of attention theoretically and experimentally. The three basic characteristics of QCD, chiral symmetry, quark confinement, and asymptotic freedom, play an important role in determining the properties of hadrons and the phase diagram at finite temperature and density [1–5]. Understanding these aspects could help us to get better knowledge of strongly interacting matter. However, the QCD equation is difficult to solve using a purely mathematical method. Specially, the larger coupling constant in the low energy regime restricts the application of perturbative QCD. On the other hand, the sign problem in Monte Carlo simulation prevents of lattice QCD simulation [6]. Consequently, more often results are phenomenologically investigated by effective models based on the spirit of QCD.

The asymptotic freedom indicates that interaction of quarks becomes weaker with decreasing distance and becomes stronger as the separation increases. It is described by a variational coupling constant or represented by a density- and temperature-dependent mass of quasiparticles in the literature [7–9]. The chiral symmetry breaking was successfully investigated in the Nambu–Jona-Lasinio (NJL) model at finite temperature by the dynamical generation of quark mass, which can act as an order parameter of chiral phase transition [10]. At high densities of a good simulation of the compact star, the deconfinement phase transition is expected to take place, which is characterized by a approximately $Z(3)$ center symmetry breaking. Phenomenologically, it has been widely realized by introducing a Polyakov potential in the NJL model at finite temperature. Consequently, the Polyakov Nambu–Jona-Lasinio (PNJL) model had long been widely employed in the investigation of the chiral phase diagram and the confinement-deconfinement transition [11–15]. However, in the conventional version of the PNJL model, the physics of confinement from the Polyakov potential would be lost at zero temperature. Recently, by introducing a Polyakov-loop-

dependent coupling strength, the deconfinement transition in the PNJL model has been improved to be operative in the zero temperature regime [16,17].

Recently, the investigation of QCD in strong magnetic fields shed new light on the whole phase diagram. The typical strength of strong magnetic fields could be of the order of 10^{12} G on the surface of pulsars. Some magnetars can have even larger magnetic fields as high as 10^{16} G at the surface [18–21] and 10^{18} or 10^{19} G in the interior of certain compact stars [22–24]. By comparing the magnetic and gravitational energies, the physical upper limit to the total neutron star is of order 10^{18} G [25,26]. And for self-bound quark stars, the limit could go higher, on the order of about 10^{20} G [24]. A realistic profile of the magnetic field distribution inside strongly magnetized neutron stars is proposed such that the magnetic fields increase relatively slowly with increasing baryon chemical potential in polynomial form instead of exponential form [27]. At the energies available at the CERN Large Hadron Collider (LHC), it is estimated a field as large as 5×10^{19} G can be produced. The higher order of 10^{25} G might have occurred during the electroweak phase transition in the early universe. But how strong the central magnetic field could be in compact star is an open question, which depends on the constraint of the parallel pressure of the system.

This paper is organized as follows. In Sec. II, we present the thermodynamics of the asymmetric magnetized quark matter in the SU(2) PNJL0 model. In Sec. III, the numerical results for the chiral restoration and deconfinement phase transition of isospin asymmetric matter are shown in both uniform and nonuniform magnetic fields. The last section is a short summary.

II. THERMODYNAMICS OF PNJL MODEL AT ZERO TEMPERATURE

Following the work in the SU(2) version of the PNJL model, the Lagrangian density in a strong magnetic field is

given by [16,28]

$$\mathcal{L} = \mathcal{L}_0 + \mathcal{L}_1 + \mathcal{L}_2 + \mathcal{L}_v - \mathcal{U}(\Phi, \bar{\Phi}, T) \quad (1)$$

with a free part

$$\mathcal{L}_0 = \bar{\psi}(i\gamma_\mu D^\mu - m)\psi \quad (2)$$

and a vector interaction part

$$\mathcal{L}_v = -G_v(\bar{\psi}\gamma_\mu\psi)^2 \quad (3)$$

and two different scalar interaction parts (see, e.g., [29–31])

$$\mathcal{L}_1 = G_{s1}[(\bar{\psi}\psi)^2 + (\bar{\psi}\bar{\tau}\psi)^2 + (\bar{\psi}i\gamma_5\psi)^2 + (\bar{\psi}i\gamma_5\bar{\tau}\psi)^2], \quad (4)$$

$$\mathcal{L}_2 = G_{s2}[(\bar{\psi}\psi)^2 - (\bar{\psi}\bar{\tau}\psi)^2 - (\bar{\psi}i\gamma_5\psi)^2 + (\bar{\psi}i\gamma_5\bar{\tau}\psi)^2], \quad (5)$$

where ψ represents a flavor isodoublet (u and d quarks) and $\bar{\tau}$ are isospin Pauli matrices. The coupling of the quarks to the electromagnetic field is introduced by the covariant derivative $D_\mu = \partial_\mu - ieQA_\mu$, where $Q = \text{diag}(q_u, q_d) = \text{diag}(2/3, -1/3)$ is the quark electric charge matrix. The interaction is invariant under $SU_L(2) \times SU_R(2) \times U_V(1)$ transformations. \mathcal{L}_1 exhibits an additional $U_A(1)$ symmetry, whereas this is not true for \mathcal{L}_2 . \mathcal{L}_2 has the structure of a 't Hooft determinant in flavor space [32]. This interaction can be interpreted as being induced by instantons and reflects the $U_A(1)$ anomaly of QCD. If we choose $G_{s1} = G_{s2} = G_s/2$, the Lagrangian density will recover the conventional version of the PNJL model. In this work, our study focuses on the flavor mixing and the instanton effects by defining adjustable coupling constants dependent on a parameter α as [31,33]

$$G_{s1} = (1 - \alpha)G_s, \quad G_{s2} = \alpha G_s. \quad (6)$$

We now want to study the properties of the asymmetric system at zero temperature. The up and down quark chemical

potentials

$$\mu_u = \mu + \delta\mu, \quad \mu_d = \mu - \delta\mu \quad (7)$$

are in general different. Here $\mu = \mu_B/3$ is the quark number chemical potential and $\delta\mu = \mu_I/2$ is proportional to the isospin chemical potential.

The choice of potential for the deconfinement order parameter as a function of temperature and chemical potential allows us to construct a realistic phase diagram. In the literature, the Polyakov potential $\mathcal{U}(\Phi, \bar{\Phi}, T)$ drives the phase transition from the color confined to the color deconfined phase at finite temperature. In order to extend the confinement description to zero temperature, we take $\Phi = \bar{\Phi}$ for the nonzero quark chemical potentials at the mean-field approximation. The total thermodynamical potential density for the two-flavor isospin asymmetric quark matter in the mean-field approximation reads

$$\Omega_{\text{PNJL}} = \sum_{i=u,d} \Omega_i + 2G_{s1}(\sigma_u^2 + \sigma_d^2) + 4G_{s2}\sigma_u\sigma_d - G_v(\rho_u + \rho_d)^2 + \mathcal{U}(\Phi, T) \quad (8)$$

by introducing the constituent dynamical mass M_i and renormalized chemical potential $\tilde{\mu}_i$:

$$M_i = m_i - 4G_{s1}\sigma_i - 4G_{s2}\sigma_j, \quad i \neq j \in u, d \quad (9)$$

$$\tilde{\mu}_i = \mu_i - 2G_v\rho. \quad (10)$$

The first term Ω_i is defined as $\Omega_i = \Omega_i^{\text{vac}} + \Omega_i^{\text{mag}} + \Omega_i^{\text{med}}$. At $T = 0$, the vacuum, magnetic field, and medium contributions to the thermodynamical potential are [34–36]

$$\Omega_i^{\text{vac}} = \frac{N_c}{8\pi^2} \left[M_i^4 \ln \left(\frac{\Lambda + \sqrt{M_i^2 + \Lambda^2}}{M_i} \right) - \Lambda \sqrt{M_i^2 + \Lambda^2} (M_i^2 + 2\Lambda^2) \right], \quad (11)$$

$$\Omega_i^{\text{mag}} = -\frac{N_c|q_i B|^2}{2\pi^2} \left[\zeta'(-1, x_i) - \frac{1}{2}(x_i^2 - x_i) \ln(x_i) + \frac{x_i^2}{4} \right], \quad (12)$$

$$\Omega_i^{\text{med}} = -\frac{|q_i|B}{2\pi^2} \int_0^{p_z^F} 3(\tilde{\mu}_i - E_{ni}) dp = -\frac{N_c|q_i|B}{4\pi^2} \sum_{n=0}^{n_i^{\text{max}}} \alpha_n \left\{ \tilde{\mu}_i \sqrt{\tilde{\mu}_i^2 - M_{ni}^2} - M_{ni}^2 \ln \left[\frac{\tilde{\mu}_i + \sqrt{\tilde{\mu}_i^2 - M_{ni}^2}}{M_{ni}} \right] \right\}, \quad (13)$$

where $x_i = \frac{M_i^2}{2|q_i|B}$, $E_{ni} = \sqrt{M_{ni}^2 + p_z^2}$, $M_{ni} = \sqrt{M_i^2 + 2n|q_i|B}$, and the color degenerate factor 3 is recovered once more due to the decoupling of the color interaction with the Polyakov potential. The spin degeneracy factor $\alpha_n = 2 - \delta_{n0}$ is 1 for the lowest Landau level (LLL) and 2 for higher Landau levels. At zero temperature, the occupied Landau levels have the maximum value $n_i^{\text{max}} = \frac{\tilde{\mu}_i^2 - M_i^2}{2|q_i|B}$. The condensation contribution from the quark with flavor i is

$$\sigma_i = \sigma_i^{\text{vac}} + \sigma_i^{\text{mag}} + \sigma_i^{\text{med}}. \quad (14)$$

The terms σ_i^{vac} , σ_i^{mag} , and σ_i^{med} represent the vacuum, magnetic field, and medium contributions to the quark condensation at zero temperature, respectively [34–36]:

$$\sigma_i^{\text{vac}} = -\frac{M_i N_c}{2\pi^2} \left[\Lambda \sqrt{\Lambda^2 + M_i^2} - M_i^2 \ln \left(\frac{\Lambda + \sqrt{\Lambda^2 + M_i^2}}{M_i} \right) \right], \quad (15)$$

$$\sigma_i^{\text{mag}} = -\frac{M_i |q_i| B N_c}{2\pi^2} \left\{ \ln[\Gamma(x_i)] - \frac{1}{2} \ln(2\pi) + x_i - \frac{1}{2} (2x_i - 1) \ln(x_i) \right\}, \quad (16)$$

$$\sigma_i^{\text{med}} = \frac{M_i |q_i| B N_c}{2\pi^2} \sum_{n_i=0}^{\infty} \alpha_{n_i} \int_0^{\infty} \frac{dp_z}{E_{ni}} \Theta(\tilde{\mu}_i - E_{ni}) = \frac{M_i |q_i| B N_c}{2\pi^2} \sum_{n_i=0}^{n_i^{\text{max}}} \alpha_{n_i} \ln \left(\frac{\tilde{\mu}_i + \sqrt{\tilde{\mu}_i^2 - M_{ni}^2}}{M_{ni}} \right). \quad (17)$$

We associated the chiral condensate with quark-antiquark pairs and considered it as a constant. In Ref. [37], it is declared that the energy separation between quarks and antiquarks grows so that it is no longer energetically favorable to excite antiquarks from the Dirac sea to form pairs with the quarks at the Fermi surface. On the other hand, pairs of quarks and holes with parallel momenta were suggested to be energetically favorable and give rise to the so-called inhomogeneous chiral condensates. More recently, one particular inhomogeneous phase, the so-called dual chiral density wave (DCDW), was characterized by a spatially modulated chiral condensation in both scalar and pseudoscalar channels [37,38]. Such situations are not included in this study.

The simple polynomial form for the Polyakov potential was improved by replacing the higher order polynomial term with a logarithmic form [39–41]. At finite temperature, the following ansatz is suggested [42,43]:

$$\mathcal{U}(\mu, \Phi) = (a_0 T^4 + a_1 \mu^4 + a_2 T^2 \mu^2) \Phi^2 + a_3 T_0^4 \ln(1 - 6\Phi^2 + 8\Phi^3 - 3\Phi^4). \quad (18)$$

At zero temperature, we adopt

$$\mathcal{U}_0(\mu, \Phi) \equiv a_1 \mu^4 \Phi^2 + a_3 T_0^4 \ln(1 - 6\Phi^2 + 8\Phi^3 - 3\Phi^4), \quad (19)$$

where $T_0 = 190$ MeV is the critical temperature for deconfinement in the pure gauge sector, in agreement with lattice results. At zero temperature, \mathcal{U}_0 is used to assure confinement physics.

In strong magnetic fields, we employ the phenomenology of the scalar and vector interactions dependent on the traced Polyakov loop as

$$G_{s1} \rightarrow G_{s1}(1 - \Phi^2), \quad G_{s2} \rightarrow G_{s2}(1 - \Phi^2), \\ G_v \rightarrow G_v(1 - \Phi^2), \quad (20)$$

and the effective coupling interaction would vanish in the deconfined phase due to the dependence on the order parameter in Eq. (20).

Finally, the total thermodynamic potential of asymmetric matter at zero temperature is given by

$$\Omega(\mu, \Phi, B) = \sum_i \Omega_i + 2G_{s1}(\sigma_u^2 + \sigma_d^2) + 4G_{s2}\sigma_u\sigma_d - G_v\rho^2 + \mathcal{U}(\mu, \Phi, \sigma, \rho), \quad (21)$$

where

$$\mathcal{U}(\mu, \Phi, \sigma, \rho) = \mathcal{U}_0(\mu, \Phi) - 2G_{s1}\Phi^2(\sigma_u^2 + \sigma_d^2) - 4G_{s2}\Phi^2\sigma_u\sigma_d + G_v\Phi^2\rho^2. \quad (22)$$

From the thermodynamics potential one can easily obtain the quark number density $\rho = \sum_{i=u,d} \rho_i$ with the i flavor contribution

$$\rho_i = \frac{3|q_i|B}{2\pi^2} \sum_{n_i=0}^{\infty} \alpha_{n_i} \sqrt{\tilde{\mu}_i^2 - M_i^2 - 2n_i|q_i|B}. \quad (23)$$

By minimizing the thermodynamical potential with respect to the quark condensate σ_i and the Polyakov loop Φ , we have a set of the coupled gap equations [44]:

$$\frac{\partial \Omega}{\partial \sigma_i} = 0, \quad \frac{\partial \Omega}{\partial \Phi} = 0. \quad (24)$$

III. NUMERICAL RESULT

In the nonrenormalizable model, a regularization procedure is usually applied by a three-momentum noncovariant cutoff $\Lambda = 719.23$ MeV. The quark current masses as free parameters are adopted as $m_u = m_d = 4.548$ MeV. The four-fermion couplings are $G_s = 1.954/\Lambda^2$ and $G_v = 0.3G_s$ [45]. We take $\delta\mu = 30$ MeV as half of the isospin chemical potential. We adopt the parameters $a_1 = -0.05$ and $a_3 = -0.17$ for the confinement potential, guided by Ref. [16]. The presence of the vector interaction accounts for the realization of the deconfinement transition at zero magnetic field. In following subsections, the cases of uniform strong magnetic field and chemical-potential-dependent nonuniform strong magnetic field are studied.

A. Results with uniform strong magnetic field

In Fig. 1, the dynamical mass M for u and d quarks is shown as a function of the chemical potential μ at different α values in the magnetic field $B = 3 \times 10^{18}$ G. The u - and d -quark masses are marked by the solid and dashed lines, respectively. The multiple first-order transitions occur at zero temperature due to the fermion energy dependence on the Landau level. In particular, for the $\alpha = 0$ case the curve of M_d has two jumps, around $\mu = 310$ MeV and $\mu = 440$ MeV. According to Ref. [15], the critical chemical potential is defined

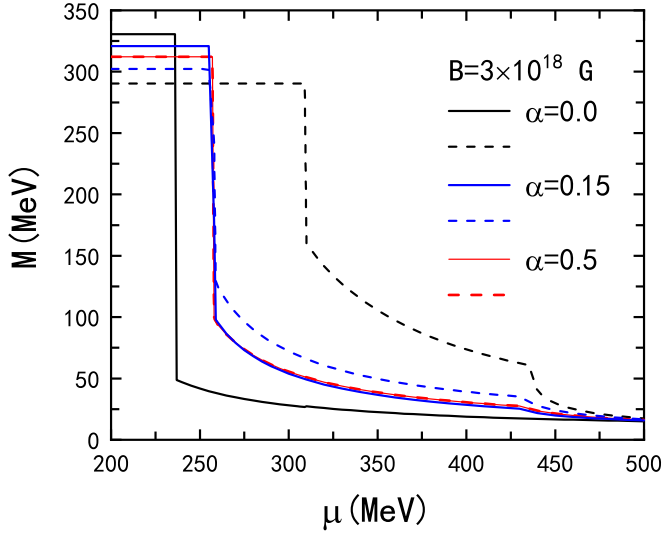


FIG. 1. The dynamical masses of u, d quarks are shown versus the chemical potential at $B = 3 \times 10^{18}$ G for different α . The u -quark masses are marked by solid lines and the d -quark masses by dashed lines.

as a threshold value, at which the order parameter decreases to half of its vacuum value. Moreover, the case $\alpha = 0$ is fully flavor decoupled, where the critical chemical potentials for the u and d quarks are mismatched. Specifically, in the range of $237 < \mu < 310$ MeV, the u quark is chirally restored while the d quark is still chirally broken. At $\alpha = 0.5$, the quark matter is isospin symmetric so that the chiral transitions for u and d quarks take place simultaneously and the mass $M_u = M_d$ can be always maintained. In fact, as the parameter α increases up to $\alpha = 0.15$ marked by the blue lines, the u and d quarks get chiral restoration simultaneously. So the critical value α_c is available to remove the mismatch of the chiral restoration between the u and d quarks, which will be discussed later.

In Fig. 2, at the magnetic field $B = 3 \times 10^{18}$ G, the Polyakov loop Φ is shown at three different values, $\alpha = 0, 0.15, 0.5$. It is seen that all the lines almost overlap and are insensitive to α , which can be accounted for by the fact that α does not change the color structure but the flavor space. So it is expected that α has no effect on the color deconfinement transition. It can be concluded that the flavor mixing or isospin asymmetry has no effect on the deconfinement phase transition.

In Fig. 3, it is obvious that the stronger the magnetic field is, the larger the critical chemical potential μ_c^u (or μ_c^d) is, which means that the condition of chiral restoration becomes more severe in a stronger magnetic field. There exists a critical value α_c , above which the mismatch of the flavor isodoublet is removed, and the chiral phase transition occurs simultaneously and the flavor mixing effect disappears.

The parameter α can change the isospin symmetry. In general, the isospin symmetry can be broken by α away from 0.5. Correspondingly, the critical chemical potentials for u and d are different. However, the difference between the μ_c^u and μ_c^d is removed at α larger than a threshold value α_c , which is shown as a function of the magnetic field in Fig. 4.

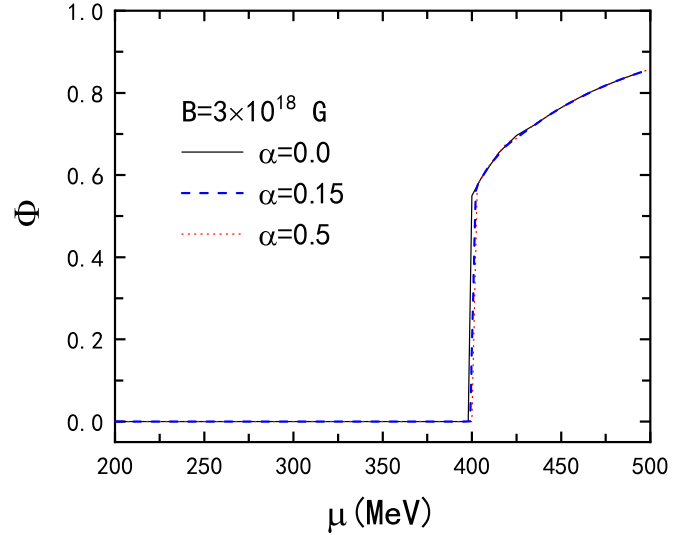


FIG. 2. The Polyakov loop is shown versus the chemical potential for different α at $B = 3 \times 10^{18}$ G.

The decreasing function demonstrates that the stronger the magnetic field is, the more likely the chiral restoration of the flavor isodoublet will happen at the common critical chemical potential. It can be concluded that the isospin symmetry structure is more favorable in the stronger magnetic field. In other words, the strong magnetic field enables the u and d quarks to be chirally restored simultaneously even at $\alpha \neq 0.5$.

B. Results with nonuniform magnetic field

In a strong magnetic field, the breaking of the rotational symmetry produces an anisotropic structure, with the parallel pressure and the transverse pressure in directions along and perpendicular to the magnetic field respectively [24,46]. Some magnetars with larger magnetic fields as high as 10^{16}

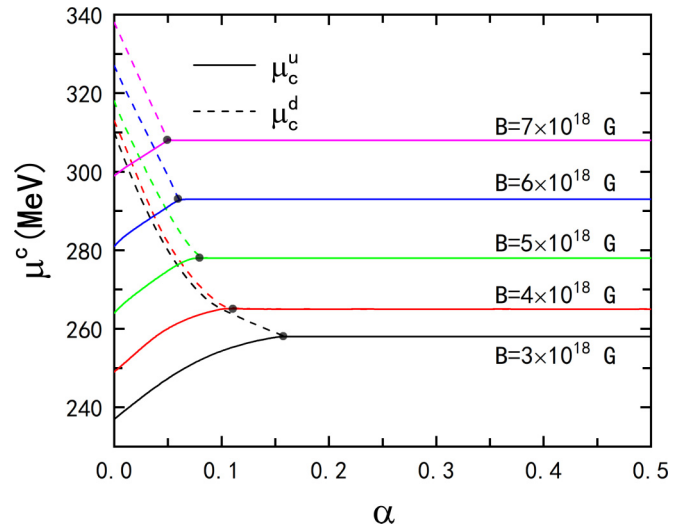


FIG. 3. The critical chemical potentials of u, d quarks are shown versus α in different magnetic fields. The solid and dashed lines denote the u and d quarks, respectively.

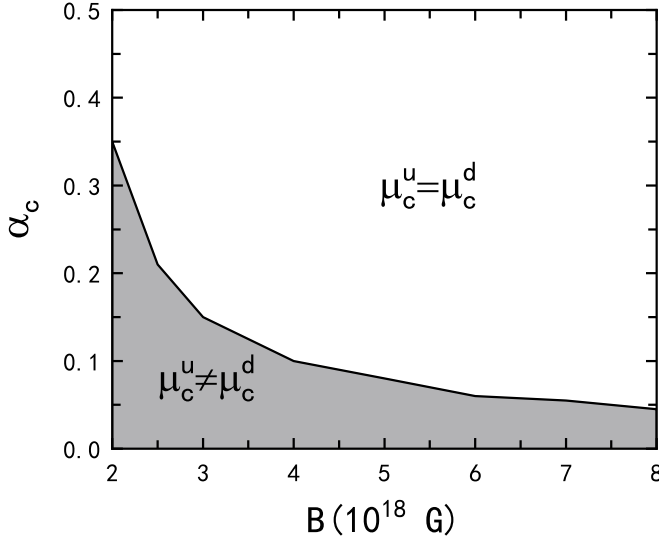


FIG. 4. The threshold value α_c for the disappearance of the mismatch between μ_c^u and μ_c^d is shown with B .

G on the surface and 10^{18} G in the interior would exhibit anisotropic structure. The anisotropic pressure was displayed by a splitting of the parallel and transverse pressures in a nonuniform magnetic field. There are some polynomial magnetic field profiles satisfying Maxwell equations [27,47], but the accuracy of these profiles in a direction other than polar and their compatibility with the presence of a non-negligible toroidal component have not yet been studied. Furthermore, these profiles are almost flat and they do not allow reaching internal magnetic field strength values much beyond the order of magnitude of the surface field [48].

We employ a magnetic field profile that is a function of the baryon chemical potential:

$$B(\mu_B) = B_s + B_c \left(1 - e^{b \frac{(\mu_B - 938)^a}{938}}\right), \quad (25)$$

where $\mu_B = 3\mu$, $a = 2.5$, $b = -4.08 \times 10^{-4}$, and $B_s = 10^{15}$ G. The value 938 MeV is the of the baryon chemical potential on the star surface. The parameters B_s and B_c correspond to the orders of magnitude of the magnetic field at the surface and the center of the star, respectively. B_c is estimated to be in the range $(0.1-4.2) \times 10^{18}$ G according to the Einstein and Maxwell equations self-consistently for non rotating and rotating stars [49,50]. Another result suggested the maximum field prevailing at the center is 5×10^{18} G [23]. And in Ref. [51], B_c is limited to $(1-3) \times 10^{18}$ G. In our work, we take the values of B_c ranging $(2-4) \times 10^{18}$ G.

In this calculation, the matter pressure should be normalized by considering the zero pressure condition at the critical point. So we have the normalized term [33,52]

$$\Delta P = -\Omega(\mu, \Phi, B) + \Omega(\mu_0, \Phi_0, B). \quad (26)$$

Under strong magnetic fields, the total pressure of the system should be a sum of the matter pressure and the field pressure contributions. Then we have parallel and transverse

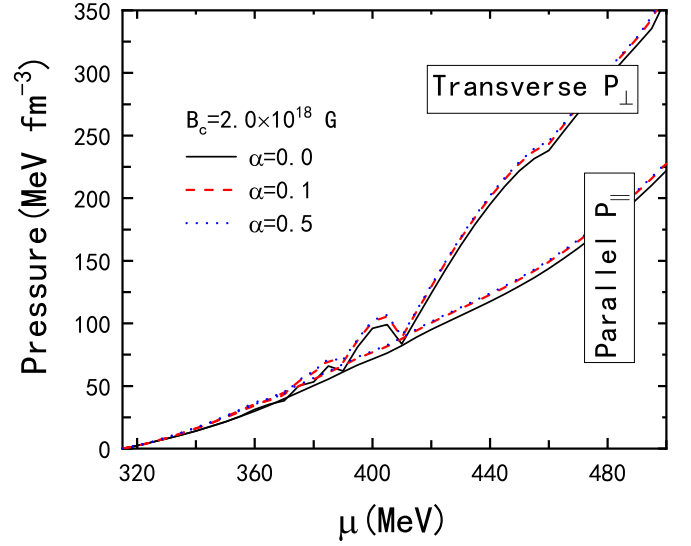


FIG. 5. Anisotropic pressure in a nonuniform magnetic field $B(\mu_B)$ at the central value $B_c = 2.0 \times 10^{18}$ G.

pressures [53–57]

$$P_{\parallel} = \Delta P - \frac{B^2}{8\pi}, \quad (27)$$

$$P_{\perp} = \Delta P - \mathcal{M}B + \frac{B^2}{8\pi}, \quad (28)$$

where the magnetic susceptibility reads [36,58]

$$\mathcal{M} = - \sum_i \frac{\partial \Omega_i}{\partial B}. \quad (29)$$

We investigate the anisotropic pressure of isospin asymmetric quark matter in a nonuniform magnetic field at zero temperature.

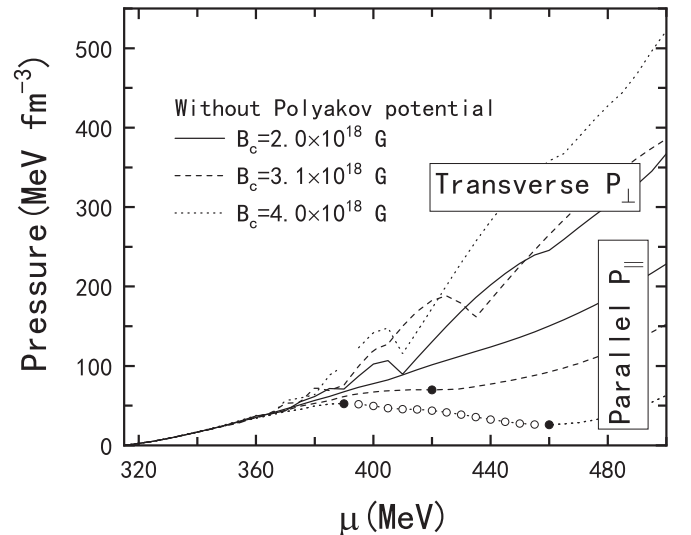


FIG. 6. Anisotropic pressure in a nonuniform magnetic field without the Polyakov potential.

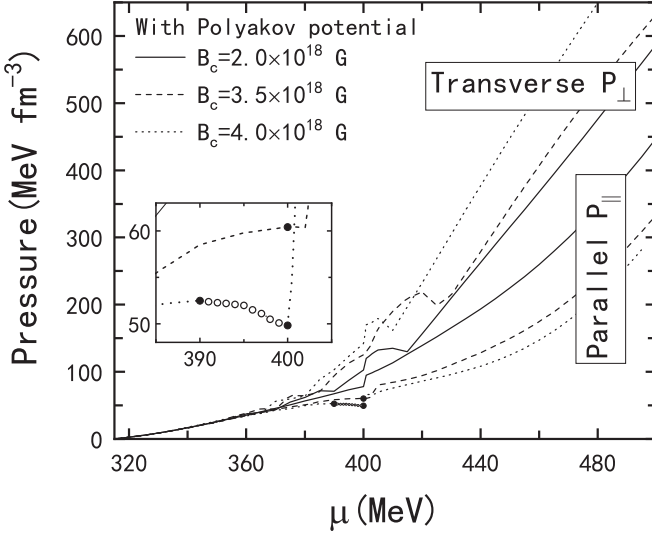


FIG. 7. Same as Fig. 6 but with the Polyakov potential.

In Fig. 5, we plot the anisotropic pressures P_{\parallel} and P_{\perp} as functions of μ at $B_c = 2 \times 10^{18}$ G with different α . The parallel pressure P_{\parallel} increases monotonically with μ , while the transverse pressure P_{\perp} oscillates due to the oscillations of the magnetization \mathcal{M} . It is known as the de Haas–van Alphen effect due to the change of Landau energy level in the magnetic field [59–61]. It was predicted for the first time by Landau and then was confirmed experimentally in some metals [61,62]. In Ref. [63], the magnetization oscillations are changed by the magnetic field and become slower as the magnetic field increases. The nonuniform magnetic field in Eq. (25) increases as the chemical potential increases. Therefore, the transverse pressure tends to oscillate slowly at high densities. At low chemical potentials, the amplitude of the oscillations is small. Both P_{\parallel} and P_{\perp} are insensitive to α . Therefore, the effect of α on the anisotropic pressure can be ignored.

In Figs. 6 and 7, P_{\parallel} and P_{\perp} are plotted for different central magnetic fields B_c at $\alpha = 0.5$. It can be seen that the transverse pressure P_{\perp} increases as the central magnetic field increases, while the parallel pressure P_{\parallel} decreases. The anisotropic structure is obviously enhanced by the increasing central magnetic field. As the central magnetic field changes, the monotonically increasing P_{\parallel} turns into a nonmonotonic function of μ . This is due to the competition of the two factors affecting the pressure behavior, namely, the positive matter (chemical potential) contribution and the negative magnetic field contribution. If the field contribution overwhelms the matter contribution to the pressure, $\partial P_{\parallel}/\partial \mu < 0$ appears. This results from the chemical-potential-dependent magnetic field $B(\mu_B)$ in Eq. (25). It indicates that the selected ansatz has this peculiarity rather than a signal that violates the general self-consistency. At $B_c = 4.0 \times 10^{18}$ G, the descending behavior of P_{\parallel} in the region between two points is unstable according to the mathematical characteristic of the selected ansatz. This

indicates the existence of a maximum central magnetic field B_c^{\max} at which the derivative $\partial P_{\parallel}/\partial \mu = 0$, marked by a full dot on the dashed line. Without the Polyakov potential in Fig. 6, the maximum value of the central magnetic field is determined as $B_c^{\max} = 3.1 \times 10^{18}$ G. By introducing the Polyakov potential at zero temperature in our model, we can obtain an enlarged central magnetic field $B_c^{\max} = 3.5 \times 10^{18}$ G as shown in Fig. 7.

IV. CONCLUSION

In this paper, we have employed the PNJL0 model to investigate isospin-asymmetric matter at zero temperature, which is realized by altering the fraction parameter α of the scalar coupling and the instanton-induced interaction. At $\alpha = 0.5$ for the isospin symmetry state, the chiral phase transitions of u and d flavors occur simultaneously with $M_u = M_d$. At $\alpha = 0$ for the strong isospin asymmetry state, the chiral transition is accompanied by the discrepancy of the flavor isodoublet, where the u quark gets chirally restored first. We have found that there is a threshold value α_c , above which the chiral transition for the u and d quarks takes place simultaneously. The simultaneous phase transition happens even if their masses are not equal. Moreover, α_c would be decreased by increasing magnetic field. Therefore, it could be concluded that the simultaneous phase transition for isospin asymmetric matter tends to be more favorable in a stronger magnetic field.

The isospin asymmetry in flavor space is usually available in compact stars. It has been numerically demonstrated that the parameter α has no effect on the color deconfinement transition, as expected. By introducing a nonuniform magnetic field to simulate these realistic environments of compact stars, it has been found that the presence of the Polyakov potential would yield the maximum central magnetic field B_c^{\max} from 3.1×10^{18} to 3.5×10^{18} G. The Polyakov potential will have an important effect on the equation of state and consequently on how strong a central magnetic field the compact star could accommodate in the interior.

It was shown in Ref. [64] that the presence of a magnetic field favors the formation of spatially inhomogeneous condensate configurations at low temperatures and nonzero chemical potential. More realistic systems should be considered in the magnetic field that is named the magnetic dual chiral density wave (MDCDW) [65]. It would be of some interest to extend our present work to more realistic systems, where the chiral condensate is associated with a hole-particle pair in the MD-CDW phase.

ACKNOWLEDGMENTS

The authors would like to acknowledge support from the National Natural Science Foundation of China under Grants No. 11875181 and No. 11705163. This work was also sponsored by the Fund for Shanxi “1331 Project” Key Subjects Construction.

- [1] E. S. Abers and B. W. Lee, *Phys. Rep.* **9**, 1 (1973).
- [2] D. J. Gross and F. Wilczek, *Phys. Rev. Lett.* **30**, 1343 (1973).
- [3] M. E. Peskin and D. V. Schroeder, *An Introduction To Quantum Field Theory* (Addison-Wesley, Reading, MA, 1995).
- [4] A. W. Thomas and W. Weise, *The Structure of the Nucleon* (Wiley, New York, 2001).
- [5] H. Satz, *Extreme States of Matter in Strong Interaction Physics: An Introduction*, Lecture Notes in Physics Vol. 841 (Springer, Berlin, 2012), pp. 1–239.
- [6] G. P. Lepage and P. B. Mackenzie, *Phys. Rev. D* **48**, 2250 (1993).
- [7] P. Levai and U. W. Heinz, *Phys. Rev. C* **57**, 1879 (1998).
- [8] P. Chakraborty and J. I. Kapusta, *Phys. Rev. C* **83**, 014906 (2011).
- [9] S. Plumari, W. M. Alberico, V. Greco, and C. Ratti, *Phys. Rev. D* **84**, 094004 (2011).
- [10] Y. Nambu and G. Jona-Lasinio, *Phys. Rev.* **122**, 345 (1961).
- [11] A. M. Polyakov, *Phys. Lett. B* **72**, 477 (1978).
- [12] L. Susskind, *Phys. Rev. D* **20**, 2610 (1979).
- [13] B. Svetitsky and L. G. Yaffe, *Nucl. Phys. B* **210**, 423 (1982).
- [14] B. Svetitsky, *Phys. Rep.* **132**, 1 (1986).
- [15] M. Ferreira, P. Costa, and C. Providência, *Phys. Rev. D* **97**, 014014 (2018).
- [16] O. A. Mattos, T. Frederico, and O. Lourenço, *Eur. Phys. J. C* **81**, 24 (2021).
- [17] O. A. Mattos, T. Frederico, C. H. Lenzi, M. Dutra, and O. Lourenço, *Phys. Rev. D* **104**, 116001 (2021).
- [18] G. Chanmugam, *Annu. Rev. Astron. Astrophys.* **30**, 143 (1992).
- [19] P. Møller, S. J. Warren, S. M. Fall, J. U. Fynbo, and P. Jakobsen, *Astrophys. J.* **574**, 51 (2002).
- [20] B. Paczynski, *Acta Astron.* **42**, 145 (1992).
- [21] A. I. Ibrahim, C. B. Markwardt, J. H. Swank, S. Ransom, M. Roberts, V. Kaspi, P. M. Woods, S. Safi-Harb, S. Balman, W. C. Parke *et al.*, *AIP Conf. Proc.* **714**, 294 (2004).
- [22] S. Chakraborty, D. Bandyopadhyay, and S. Pal, *Phys. Rev. Lett.* **78**, 2898 (1997).
- [23] D. Bandyopadhyay, S. Chakraborty, and S. Pal, *Phys. Rev. Lett.* **79**, 2176 (1997).
- [24] E. J. Ferrer, V. de la Incera, J. P. Keith, I. Portillo, and P. L. Springsteen, *Phys. Rev. C* **82**, 065802 (2010).
- [25] D. Lai and S. L. Shapiro, *Astrophys. J.* **383**, 745 (1991).
- [26] I. S. Suh and G. J. Mathews, *Astrophys. J.* **546**, 1126 (2001).
- [27] V. Dexheimer, B. Franzon, R. O. Gomes, R. L. S. Farias, S. S. Avancini, and S. Schramm, *Phys. Lett. B* **773**, 487 (2017).
- [28] H. Hansen, W. M. Alberico, A. Beraudo, A. Molinari, M. Nardi, and C. Ratti, *Phys. Rev. D* **75**, 065004 (2007).
- [29] M. Asakawa and K. Yazaki, *Nucl. Phys. A* **504**, 668 (1989).
- [30] S. P. Klevansky, *Rev. Mod. Phys.* **64**, 649 (1992).
- [31] M. Frank, M. Buballa, and M. Oertel, *Phys. Lett. B* **562**, 221 (2003).
- [32] G. 't Hooft, *Phys. Rep.* **142**, 357 (1986).
- [33] L. Yang and X. J. Wen, *Int. J. Mod. Phys. A* **33**, 1850123 (2018).
- [34] D. P. Menezes, M. Benghi Pinto, S. S. Avancini, and C. Providência, *Phys. Rev. C* **80**, 065805 (2009).
- [35] S. S. Avancini, D. P. Menezes, and C. Providência, *Phys. Rev. C* **83**, 065805 (2011).
- [36] D. P. Menezes, M. B. Pinto, and C. Providência, *Phys. Rev. C* **91**, 065205 (2015).
- [37] E. J. Ferrer and V. de la Incera, *Nucl. Phys. B* **931**, 192 (2018).
- [38] A. Candeloro, C. Degli Esposti Boschi, and M. G. A. Paris, *Phys. Rev. D* **102**, 056012 (2020).
- [39] K. Fukushima, *Phys. Lett. B* **591**, 277 (2004).
- [40] S. Rößner, T. Hell, C. Ratti, and W. Weise, *Nucl. Phys. A* **814**, 118 (2008).
- [41] S. Rößner, C. Ratti, and W. Weise, *Phys. Rev. D* **75**, 034007 (2007).
- [42] V. A. Dexheimer and S. Schramm, *Nucl. Phys. A* **827**, 579C (2009).
- [43] V. A. Dexheimer and S. Schramm, *Phys. Rev. C* **81**, 045201 (2010).
- [44] M. Buballa, *Phys. Rep.* **407**, 205 (2005).
- [45] S. S. Avancini, R. L. S. Farias, N. N. Scoccola, and W. R. Tavares, *Phys. Rev. D* **99**, 116002 (2019).
- [46] E. J. Ferrer and A. Hackebill, *Int. J. Mod. Phys. A* **37**, 2250048 (2022).
- [47] D. Chatterjee, J. Novak, and M. Oertel, *Phys. Rev. C* **99**, 055811 (2019).
- [48] M. O. Celi, M. Mariani, M. G. Orsaria, and L. Tonetto, *Universe* **8**, 272 (2022).
- [49] M. Bocquet, S. Bonazzola, E.ourgoulhon, and J. Novak, *Astron. Astrophys.* **301**, 757 (1995).
- [50] C. Y. Cardall, M. Prakash, and J. M. Lattimer, *Astrophys. J.* **554**, 322 (2001).
- [51] A. E. Broderick, M. Prakash, and J. M. Lattimer, *Phys. Lett. B* **531**, 167 (2002).
- [52] H. Liang and X. J. Wen, *Int. J. Mod. Phys. A* **34**, 1950170 (2019).
- [53] V. R. Khalilov, *Phys. Rev. D* **65**, 056001 (2002).
- [54] A. A. Isayev and J. Yang, *J. Phys. G* **40**, 035105 (2013).
- [55] A. A. Isayev and J. Yang, *Phys. Lett. B* **707**, 163 (2012).
- [56] A. A. Isayev and J. Yang, *Phys. Rev. C* **84**, 065802 (2011).
- [57] A. A. Isayev, *Phys. Rev. D* **98**, 043022 (2018).
- [58] S. S. Avancini, V. Dexheimer, R. L. S. Farias, and V. S. Timóteo, *Phys. Rev. C* **97**, 035207 (2018).
- [59] D. P. Menezes, M. Benghi Pinto, S. S. Avancini, A. Pérez Martínez, and C. Providência, *Phys. Rev. C* **79**, 035807 (2009).
- [60] V. A. Miransky and I. A. Shovkovy, *Phys. Rep.* **576**, 1 (2015).
- [61] D. Ebert, K. G. Klimenko, M. A. Vdovichenko, and A. S. Vshivtsev, *Phys. Rev. D* **61**, 025005 (1999).
- [62] W. J. de Haas and P. M. van Alphen, *Proc. Am. Acad. Arts Sci.* **33**, 1106 (1936).
- [63] J. O. Andersen and T. Haugset, *Phys. Rev. D* **51**, 3073 (1995).
- [64] I. E. Frolov, V. C. Zhukovsky, and K. G. Klimenko, *Phys. Rev. D* **82**, 076002 (2010).
- [65] E. J. Ferrer and V. de la Incera, *Phys. Lett. B* **769**, 208 (2017).